Running Head: *Alkenone Production at Station ALOHA*

Seasonal Patterns of Alkenone Production in the Subtropical Oligotrophic North Pacific

Brian N. Popp[1], Fredrick G. Prahl[2], Richard J. Wallsgrove[3] and Jamie Tanimoto[1]

[1]Department of Geology & Geophysics, University of Hawaii, Honolulu, HI
[2]College of Oceanic and Atmospheric Sciences, Oregon State University, Corvallis, OR
[3]Department of Oceanography, University of Hawaii, Honolulu, HI

Revised copy to *Paleoceanography*

Index Terms: 4267 Oceanography: General: Paleoceanography; 4850 Oceanography: Biological and Chemical: Organic marine chemistry; 4855 Oceanography: Biological and Chemical: Plankton; 4808 Oceanography: Biological and Chemical: Chemical tracers; 1615 Global Change: Biogeochemical processes (4805); **Keywords:** alkenone unsaturation index, alkenone concentration, alkenone production rate, paleotemperature proxy, biomarker.

1. Abstract

Seasonal alkenone concentrations, production rates and unsaturation patterns ($U^{K'}_{37}$) were measured at Station ALOHA in the oligotrophic subtropical North Pacific. Highest alkenone concentration and production rates were found in (winter, fall) or just below (summer) the surface mixed layer. Lowest alkenone concentration and production rates were found within the deep chlorophyll maximum layer (DCML). In the DCML, which occurs at 80-120 m throughout the year, $U^{K'}_{37}$-temperatures overestimated water temperatures by ~2-4°C. This result probably reflected the effect of light limitation on the physiology of alkenone producing algae. At the depth of maximum alkenone production, $U^{K'}_{37}$-temperatures underestimated water temperature by ~2-4ºC in summer and fall but overestimated *in situ* temperatures by ~1-2ºC in winter. The underestimate of measured water temperature in summer and fall most likely reflected a physiological response to limited nutrient availability. The $U^{K'}_{37}$-temperature overestimate in winter was best explained by a change in the ecology of alkenone-producing algae.

2. Introduction

[1] C_{37-39} alkenones are biosynthesized by a select set of haptophyte algae, the most notable example being *Emiliania huxleyi* [*Brassell,* 1993]. *E. huxleyi* is eurythermal and consequently, found widely distributed in surface waters throughout the world ocean. Alkenone unsaturation patterns vary directly with algal growth temperature [*Conte et al.,* 1998], which underpins use of the $U^{K'}_{37}$ index for paleothermometry [*Brassell et al.,* 1986]. Alkenone unsaturation patterns are thus now widely analyzed by the paleoceanographic community for reconstruction of sea surface temperature [*e.g., Prahl et al.,* 2000].

[2] Statistical calibration derived from analysis of alkenone unsaturation patterns in a large collection of core top sediments from the global ocean shows a significant linear correlation between $U^{K'}_{37}$ and mean annual sea-surface temperature (maSST) [*Muller et al.,* 1998]. This

calibration agrees well with the first formal evaluation of cultures that showed $U^{K'}_{37}$ varied linearly with growth temperature ($\equiv 0.034T + 0.039$; $r^2 = 0.97$, Clone CCMP 1742) over the range 8-25°C [*Prahl et al.*, 1988]. This agreement indicated the culture calibration clearly applied to the open ocean [*Prahl and Wakeham*, 1987]. Although these empirical findings justify use of $U^{K'}_{37}$ for estimating paleotemperature, the global calibration of *Muller et al.* [1998] displays considerable, yet unexplained scatter of up to ±3°C around any specific $U^{K'}_{37}$ measurement. Therefore, there is reason for concern about the accuracy of reconstructed maSST through geologic time using global calibrations for $U^{K'}_{37}$.

[3] Scatter in the global calibration could be caused by geological as well as non-diagenetic biological factors [*Prahl et al.*, 2003]. Scatter caused by inclusion of sedimentary samples of non-Modern age (a geological factor) is perhaps not a serious concern and could be eliminated through use of compound specific radiocarbon dating techniques [*Ohkouchi et al.,* 2002]. However, contribution to the scatter by non-diagenetic biological factors is a more critical issue for which there is as yet no obvious resolution.

[4] A significant fraction of the scatter in the global calibration may also reflect ecological, genetic and non-thermal biological factors affecting alkenone-producing algae that are not readily apparent when $U^{K'}_{37}$ is simply equated statistically to maSST. For example, subsurface production within the euphotic zone could potentially be an important source of alkenones preserved in sediments (e.g., see *Prahl et al.* [2005] and references therein). Alkenone-based temperatures would underestimate surface mixed layer (SML) temperatures if alkenone-producing algae lived within the thermocline and most of the signal recorded in sediments was exported from that water column location. There is also interest in reconstructing climatic variation in atmospheric pCO_2 from down core stratigraphic analysis of alkenones in marine sediments [*Pagani et al.* 1999; 2002]. The success of this application requires knowledge of where in the euphotic zone this biomarker signal preserved in sediment is produced. If the signal does not originate primarily from the SML, then algal growth in equilibrium with atmospheric pCO_2 is unlikely.

[5] Biological factors can also potentially contribute to scatter in the global calibration. Not all alkenone-producing algae isolated from the ocean display the same $U^{K'}_{37}$ response to growth temperature [*Conte et al*., 1998]. In addition, alkenone unsaturation can be influenced by environmental properties other than growth temperature such as nutrient and light availability [*Epstein et al*., 1998; 2001; *Versteegh et al*., 2001; *Prahl et al*., 2003]. One goal of our present work is to evaluate the extent that scatter in the global calibration might reflect influence from these ecological, genetic and non-thermal physiological factors.

[6] In this paper, we evaluate how alkenone concentration, production rates and unsaturation patterns vary with upper water column depth (0 to ~160m) and season (summer, fall, winter) at Station ALOHA in the oligotrophic subtropical North Pacific gyre near Hawaii. Alkenone production rate was determined using an *in situ* ^{13}C incubation method modified after that employed previously in the Sea of Japan [*Hamanaka et al*., 2000] and the Bering Sea [*Shin et al*., 2002]. We test our improved method using laboratory culture experiments. We also evaluate how significantly alkenone-producing algae contribute to the haptophyte biomass in these waters. We show that this assessment can be done using a simple algorithm based on new observational data from culture experiments. We found that the alkenone-producing algae contributed very little to the overall hayptophyte biomass at Station ALOHA even though measurable alkenone concentrations were found in the water column throughout the year. Alkenone concentrations and production rates were at all times greatest within or just below the SML. Lowest alkenone concentrations and production rates were consistently found at the depth of the deep chlorophyll maximum layer (DCML, *sensu Longhurst and Harrison* [1989]), a year round persistent feature of the euphotic zone at Station ALOHA. Measured $U^{K'}_{37}$ values when converted into growth temperature estimates did not always match actual water temperatures at the depth of sample collection. These results are discussed in terms of the ecological and non-thermal, physiological factors that can influence alkenone unsaturation patterns in the central oligotrophic North Pacific.

3. Sampling and Analytical Methods

3.1 Sample Site Characteristics

[7] Samples were collected from the Hawaii Ocean Time-series (HOT) Station ALOHA (22˚45'N, 158˚W; *Karl and Lukas* [1996]) on three different cruises: KOK-0111 (16-23 July 2001), HOT-131 (21-26 October 2001) and KOK-0303 (17-22 February 2003). KOK-0111 occurred just after HOT-128 (9-13 July 2001) and KOK-0303 occurred just before HOT-145 (24-28 February 2003), thus applicable ancillary data are available from these cruises. All cruises were aboard the *R/V Kaimikai-o-Kanaloa*. Station ALOHA is located 100 km north of the island of Oahu and has a total water column depth of 4700 m.

[8] Water column profiles of photosynthetic active radiation (PAR) were calculated assuming exponential decrease in PAR with increasing water depth, i.e.

$$PAR = ae^{-k_{PAR}z}. \quad (1)$$

In eqn. 1, a is surface PAR, z is depth below the sea-surface and k_{PAR} is the seasonal light attenuation coefficient determined for Station ALOHA [*Letelier et al*., 2004]. Surface PAR, measured using a PRR-610 surface reference radiometer (Biospherical Instruments), is available for most 1998-2004 HOT cruises (http://hahana.soest.hawaii.edu/hot/hot-dogs/prrseries.html). The wintertime k_{PAR} (0.044 m^{-1}) and the measured surface PAR were used to calculate PAR as a function of depth for HOT-131. We used the wintertime k_{PAR} and the average surface PAR measured during HOT-144 (15-19 January 2005) and HOT-145 to calculate the PAR depth profile for KOK-0303. Surface PAR was not measured during HOT-128. Consequently, the depth profile for PAR during our summer cruise (KOK-0111) was assessed using the average July surface PAR for 2000-2004 assuming the *Letelier et al*. [2004] summer bloom k_{PAR} value (0.0525 m^{-1}). *Letelier et al*. [2004] found that surface PAR measured seasonally did not differ from that predicted for climatological sea-surface solar

irradiance using a classical astronomical formula [*Brock*, 1981] and the appropriate correction for the solar constant [*Duffie and Beckman*, 1980].

3.2 Sample Collection

3.2.1 Suspended Particulate Material and Water Sample Collection

[9] Sample collection followed the protocols and methods in our related study [*Prahl et al.*, 2005]. We present here only a brief description and refer the reader to that publication for further details. Suspended particulate material (SPM) for alkenone analysis was obtained on glass-fiber filters (GF/F) using Challenger Oceanic *in situ* high volume pumps. The depth of *in situ* sample collection was estimated on KOK-0111 from temperature data obtained using a logger attached to each pump that was subsequently referenced to CTD profile data. On HOT-131 and KOK-0303, the depth of *in situ* sample collection was determined directly using data obtained from a temperature-pressure recorder deployed with the pump cast. SPM for alkenone analysis was also filtered onto GF/F from water collected using PVC sample bottles on dedicated CTD casts and at the surface (~7 m depth) using the ship's uncontaminated seawater system. Water samples were also taken from PVC sample bottles on dedicated CTD casts for determination of the isotopic composition of total dissolved inorganic carbon ($\delta^{13}C_{DIC}$).

[10] Water samples (~100 L) for incubation experiments were transferred from PVC bottles on the CTD rosette to acid cleaned 25 L polycarbonate bottles at which time ^{13}C-labeled bicarbonate was added. The bottles were then sealed and attached to an *in situ* array which was deployed during predawn hours and collected at sunrise the following day. The free-floating array design was used to replicate as closely as possible *in situ* light and temperature conditions from which the samples were collected. On KOK-0111 and KOK-0303, *in situ* experiments were also preformed to determine the effect of light limitation on the physiology of alkenone-producing algae. During KOK-0111, water collected from the depth of the

DCML (135 m) was incubated at a single depth in the SML (~25 m) while on KOK-0303, water collected from the DCML (120 m) was incubated at four euphotic depths (40, 80, 100 and 120 m). During all other experiments, water samples were incubated at the depth of sample collection targeting the surface mixed layer (SML), the DCML and two depths in the thermocline between the base of the SML and the DCML. Upon retrieval of the *in situ* array, $\delta^{13}C_{DIC}$ samples were taken from each carboy to confirm the level of isotopic enrichment. Remaining water from all four carboys was then pressure filtered sequentially through a single, precombusted GF/F and stored frozen until needed for alkenone analysis.

3.4 Culture Experiments

[11] Laboratory culture experiments were performed at the University of Hawaii (UH) to ground-truth the alkenone labeling method and at Oregon State University (OSU) to evaluate effects of nutrient and light availability on alkenone and photosynthetic pigment concentrations. Cultures of *Emiliania huxleyi* (CCMP 1742), originally isolated from the temperate northeast Pacific Ocean and obtained from the Provasoli-Guillard National Center for Culture of Marine Phytoplankton, was used for all experiments. We are not aware of any clones of *E. huxleyi* that have been isolated from the oligotrophic North Pacific gyre. Although the clone used in our experiments was not isolated from the oligotrophic North Pacific Ocean, its $U^{K'}_{37}$ response to growth temperature change [*Prahl et al.*, 1988] is indistinguishable from that found throughout the open ocean [*Muller et al.*, 1998].

[12] At UH, *E. huxleyi* cells were grown isothermally (either 15.3°C or 19.5°C) in batch culture in 4.0 L polycarbonate bottles under nutrient-replete constant saturating light (318 μEin m^{-2} s^{-1}) conditions. Each culture consisted of 3.8 L of sterilized, 0.2 μm filtered seawater that had been amended with nutrients (f/2 media). Cultures were inoculated to obtain a starting cell density of 300 cells mL^{-1}. Growth rates, determined by daily change in cell density, varied from 0.32 d^{-1} for the 15.3°C experiment to 0.47 d^{-1} for the 19.5°C experiment. Initial samples of the cultures were taken at a cell density of ~30,000 cells mL^{-1}.

Harvesting cells at this density has been found to have a minimal effect on seawater inorganic carbon chemistry [*Laws et al.*, 2001]. Once cell density reached this level, ^{13}C-labeled bicarbonate was added. Cell counts, alkalinity, total dissolved inorganic carbon (DIC) and alkenone samples were subsequently taken at regular intervals (0 and 12 hours or 0, 12, and 24 hours) to monitor the uptake of the ^{13}C label into alkenones. Cell density was determined using a Coulter Z1 dual threshold particle counter using a 50 μm aperture tube and a 3-8 μm threshold to optimize detection of these ~5 μm diameter cells.

[13] At OSU, *E. huxleyi* cells were grown isothermally (15°C) in 0.5 L Pyrex flasks containing 0.2 μm filtered seawater that had been amended with nutrients (f/2-Si media, see http://ccmp.bigelow.org/CI/CI_01e.html). Growth occurred under a 12:12 hr light:dark cycle with non-saturating irradiance (~50-60 μEin m^{-2} s^{-1}) provided by Cool-White fluorescent lights. Culture flasks were stirred by gentle swirling at the same time each day and immediately subsampled using a sterile pipette for daily determination of cell density, nitrate and phosphate concentrations, and cellular alkenone content and composition. At each time point, cell density was determined microscopically using a haemocytometer. Cells in known volumes of culture were also filtered onto two precombusted (450°C, 8 h) GF/F (25 mm diameter) using gentle vacuum and stored frozen (-80°C) until needed for alkenone and photosynthetic pigment analysis. A volume of filtrate from each sample was also collected in an acid-cleaned, 25 mL polyethylene vial and stored frozen until needed for nutrient analysis.

3.5 Analytical Techniques

[14] The method for photosynthetic pigment analysis is described elsewhere [*Prahl et al.*, 2005]. Alkenone fractions were isolated at OSU using established ultrasonic solvent extraction and silica gel column chromatographic methods [*Prahl et al.*, 1989]. The alkenone content and composition of each fraction was analyzed quantitatively by a capillary gas chromatographic approach that is calibrated using internal standards (see *Prahl et al*.

[2005] for further details). The precision of quantitative determinations was better than ±10% for alkenone concentration and ±0.01 or less for alkenone unsaturation patterns ($U^{K'}_{37}$).

[15] In preparation for compound specific carbon isotopic analysis, alkenone fractions were then saponified [*Christie,* 1973] to eliminate interference of a di-unsaturated C_{36} methyl ester with the primary targets of interest, the di- and tri-unsaturated C_{37} methyl ketones. The $\delta^{13}C$ of isotopically labeled and unlabeled alkenone samples was determined at UH by isotope-ratio-monitoring gas chromatography mass spectrometry (irmGCMS) [*Hayes et al*., 1990]. The natural abundance of ^{13}C atomic percent is required to calculate alkenone production rate (see eqn. 2). Precision of replicate irmGCMS analyses of compounds with natural abundance carbon isotope composition was found in most cases to be ±0.3‰ (±0.0003 ^{13}C atom %) or better for individual peaks containing ≥5 nmoles of carbon with no indication of bias or inaccuracy in the results. Measured precision for compounds with modest ^{13}C-enrichment (δ-values ~50-80‰) was typically less than ±1.5‰ (±0.0017 ^{13}C atom %). The modest enrichment of ^{13}C in the DIC pool (~190‰) provided a sufficiently unambiguous isotopic signal in the alkenones for determination of their production rate by irmGCMS within a 24 h incubation period.

[16] Use of irmGCMS to determine alkenone production rate is markedly different from the pioneering method employed by *Hamanaka et al.* [2000] and *Shin et al.* [2002]. These workers used chemical ionization GCMS to quantify the relative ratios of the tracer-enriched suite of molecular ion peaks to the natural molecular ion peak for the $C_{37:2}$ and $C_{37:3}$ alkenones. Their method assumed that the intrinsic ionization efficiency of the molecular ion for the unlabeled alkenone and the quasi-molecular ions for the isotopically labeled compounds were identical. Their experimental design required enrichment of the ambient DIC concentration by up to 10% with 99% pure ^{13}C-labeled bicarbonate. Our method required no more than 0.3% enrichment in the concentration of the ambient DIC pool. Analytical uncertainty for irmGCMS determination of isotopic enrichment in labeled samples is about an order of magnitude better than the uncertainty (±0.02 ^{13}C atom %) reported by

Hamanaka et al. [2000] and *Shin et al.* [2002]. In addition, we used isotopic enrichment calculated for CO_2(aq) as opposed to that measured in total dissolved inorganic carbon (see *Hamanaka et al.* [2000]) to calculate alkenone production rates since CO_2(aq) is the primary inorganic carbon substrate utilized by *E. huxleyi* [*Rost et al.*, 2003]. Changes in temperature and the distribution of carbonate species in seawater affect isotopic fractionation between DIC (mainly bicarbonate) and CO_2(aq). Although this effect is small with large additions of ^{13}C-labeled bicarbonate, with small ^{13}C additions the use of ^{13}C atom % DIC can result in significant variation in calculated production rates between oceanic sites resulting simply from changes in the ^{13}C activity in CO_2(aq) due to equilibrium isotope effects. Therefore, we calculated alkenone production rate from the change in the ^{13}C signal of the alkenones and CO_2(aq) measured after incubation using eqn. 2 (modified after *Hama et al*. [1993]):

$$\text{Production Rate} = \frac{(a_{is} - a_{ns})}{(a_{ic} - a_{ns})} \times \frac{\text{alkenone}\,(t)}{t} \qquad (2)$$

where a_{is} is the alkenone ^{13}C atom % (either $C_{37:2}$ or $C_{37:3}$) at the end of the incubation, a_{ns} is the alkenone ^{13}C atom % (either $C_{37:2}$ or $C_{37:3}$) in a concurrently collected natural (nonincubated) sample, a_{ic} is the CO_2(aq) ^{13}C atom % in the incubation bottle, alkenone (t) is the alkenone concentration at the end of the incubation and t is the length of the incubation. Alkenone turnover rate was determined by dividing the daily production rate by alkenone concentration measured at time t. The ^{13}C atom % of alkenones in natural and incubated alkenone samples was corrected for the expected 4.2‰ isotope offset between the alkenone and primary photosynthate that is associated with biosynthesis [*Popp et al.*, 1998]. Sufficient ship time was available only during KOK-0303 for replication of *in situ* production experiments at a single depth. On that cruise, replicate experiments at the depth of the DCML (120 m) yielded 0.10 and 0.14 ng L^{-1} d^{-1}. This estimate of reproducibility (±25%) is almost certainly the worst possible case since both alkenone concentration and the rate of ^{13}C uptake were low at this depth.

[17] $\delta^{13}C_{DIC}$ was determined at UH using a technique modified from *Kroopnick* [1985] (see *Laws et al*. [1995] for details). Concentrations of carbonate species were determined using

the program developed by *Lewis and Wallace* [1988]. This program (available on the www, http://cdiac.ornl.gov/oceans/co2rprt.html) calculates the concentration of CO_2(aq) from temperature, salinity, total alkalinity and the concentrations of DIC, phosphate, and silicate. Total alkalinity and the concentrations of DIC, phosphate, and silicate were collected and analyzed by HOT program personnel for HOT-131. These data were also obtained from HOT cruises (see http://hahana.soest.hawaii.edu/hot/hot-dogs/bextraction.html) occurring within 1-2 weeks of KOK-0111 and KOK-0303. The dissociation constants for carbonic and boric acids used in this calculation were from *Dickson* [1990a, b] and *Roy et al.* [1993]. Apparent constants were corrected for the effects of pressure [*Millero*, 1979]. The isotopic composition of CO_2(aq) was determined from the relative abundances of bicarbonate, carbonate, and CO_2(aq) and the temperature-fractionation relationships of *Deines et al.* [1974] and *Mook et al.* [1974]. As determined by replicate sample analysis, uncertainty in $\delta^{13}C$ estimates for CO_2(aq) was less than ±0.1‰ for natural samples and less than ±0.002 ^{13}C atom % for labeled samples. Phosphate, silicate and nitrate plus nitrite from our culture experiments were analyzed at OSU using the colorimetric techniques of *Strickland and Parsons* [1972] on an Alpkem "Flow Solution" Autoanalyzer continuous flow system.

4. Results and Discussion

4.1 Alkenone Concentration and the Contribution of Alkenone-Producers to the Haptophyte Community at ALOHA

[18] C_{37} alkenone concentrations (K_{37}, sum of di- and tri-unsaturated C_{37} ketones) were consistently high throughout the SML during HOT-131 (fall) and KOK-0303 (winter) and decreased within the upper thermocline (Fig. 1, Table 1). K_{37} concentrations during KOK-0111 (summer) were also elevated in the SML, but reached a maximum (~5-7 ng L^{-1}) below the SML (Fig. 1) within a zone of dissolved oxygen supersaturation [*Prahl et al.*, 2005], before decreasing with greater depth. The K_{37} concentrations during winter (~9-16 ng L^{-1}) in the SML were, however approximately a factor of 2-4 higher than in summer (~2-4 ng L^{-1})

and fall (~5 ng L^{-1}). Throughout the year, K_{37} concentrations at the DCML were generally quite low (~1-4 ng L^{-1}, but were up to ~10 ng L^{-1} in winter, Fig. 1, Table 1).

[19] The fact that K_{37} concentrations are generally low in the DCML and higher at shallower depths is surprising, at least on a cursory level. Throughout the year, the concentrations of 19'-hexanoyloxyfucoxanthin (19'Hex) and chlorophyll are well correlated at Station ALOHA (see *Prahl et al.* [2005] and the web archive for HOT program referenced above). 19'Hex is a carotenoid often ascribed taxonomically to haptophyte algae at Station ALOHA [*Letelier et al*., 1993] of which *E. huxleyi* and potentially other alkenone-producing coccolithophores are prominent marine members [*Green and Leadbetter*, 1994]. In addition, as noted above subsurface alkenone production within the thermocline has been suggested as a potentially important source of alkenones preserved in sediments (*Prahl et al.* [2005] and references therein). On this basis, one might expect K_{37} concentration at Station ALOHA to correlate with 19'Hex concentration and reach its maximum at the depth of the DCML. Although such correlation is not observed, this finding is perhaps not unexpected if the system is examined in finer detail. Although many haptophytes [*Jeffrey et al*., 1997; *van Lenning et al.*, 2004] as well as select dinoflagellates [*Moon-van der Staay et al.*, 2000] biosynthesize 19'Hex as a dominant carotenoid, alkenones are known to be produced in open-oceanic waters like that at Station ALOHA only by *E. huxleyi* and the closely related *Gephyrocapsa oceanica* [*Marlowe et al.*, 1984; 1990; *Brassell*, 1993; *Volkman et al*., 1995]. Thus, lack of correlation could arise if alkenone-producing algae are minor contributors to the standing stock of 19'Hex and the ecology of these organisms differs significantly from that of the major phytoplankton species contributing to the 19'Hex distribution at ALOHA. To evaluate these observations, we compared our K_{37} concentrations with prior measurements of *E. huxleyi* cell density [*Cortes et al.*, 2001] and quantitatively estimated how significantly alkenone-producing algae contribute to the haptophyte biomass using a simple algorithm calibrated using culture data.

[20] *E. huxleyi* synthesizes C_{37-39} alkenones as major biochemical components [*Pond and Harris*, 1996]. Total C_{37-39} alkenone concentrations in exponentially dividing cells are 1-2 pg cell^{-1} [*Prahl et al.*, 1988; *Conte et al.*, 1998]. Of this amount, the C_{37} alkenones represent ~50% [*Conte et al.*, 1998]. Assuming C_{37} alkenone concentrations in natural alkenone-producing populations are comparable (i.e., ~ 0.75 pg cell^{-1}), simple algebra allows conversion of measured K_{37} concentration in a given water sample into an estimate of cell density. Using this approach, K_{37} concentrations measured at Station ALOHA in the winter SML (~9-16 ng L^{-1}) yield an estimate of ~12-21 x 10^3 cells L^{-1} while K_{37} concentrations measured within the SML/thermocline in summer and fall (~2-7 ng L^{-1}) yield an estimate of ~2-9 x 10^3 cells L^{-1} (Table 1).

[21] *Cortes et al.* [2001] examined seasonal changes in coccolithophore abundance and community structure at Station ALOHA over the period 1994-96 with approximately monthly resolution. They found that *E. huxleyi* was present in most samples and when observed, comprised >20% of the community. During their three year study period, *E. huxleyi* displayed peak abundance consistently in late winter to early spring at a surface to mid-water depth within the euphotic zone, similar to features evident in our winter depth profile for K_{37} concentration (Fig. 1C). Peak abundances determined by microscopic analysis varied between years and ranged from ~6-20 x 10^3 cell L^{-1} [*Cortes et al.*, 2001]. These values are within the cell density range we estimated from K_{37} concentrations measured throughout the year (Table 1).

[22] With knowledge of 19'Hex and K_{37} concentrations in a water sample from the euphotic zone, eqn. 3 can be used to estimate the percent contribution of alkenone-producing cells to the total haptophyte community (%Hapto):

$$\%Hapto = \frac{[19'Hex/K_{37}]_{apc} \times [K_{37}]_{insitu}}{[19'Hex]_{insitu}} \times 100. \qquad (3)$$

In this equation, $[K_{37}]_{insitu}$ and $[19'Hex]_{insitu}$ are the concentrations of total C_{37} alkenones and 19'Hex measured in a water sample, respectively, and $[19'Hex/K_{37}]_{apc}$ represents the carotenoid to total C_{37} alkenone ratio of ***a***lkenone-***p***roducing ***c***ells. In batch culture experiments with *E. huxleyi*, the measured $[19'Hex/K_{37}]_{apc}$ value in exponentially growing cells is ~0.1 (Fig. 2). Results from these experiments also show the value for $[19'Hex/K_{37}]_{apc}$ is not constant but decreases to ~0.04 in stationary phase, nutrient-limited cells (Fig. 2C) and increases to ~0.3 when cells are exposed to complete darkness for multiple days (Fig. 2D). Although culture data suggests the 19'Hex quota may have some dependence on the cell's physiological status (Fig. 2C, D), the primary cause for variation in $[19'Hex/K_{37}]_{apc}$ values is alkenone accumulation in nutrient-limited stationary phase cells (K_{37} ~1.85 pg cell^{-1}) and depletion under conditions of long-term, dark stress (K_{37} ~0.25 pg cell^{-1}) (Fig. 2, see also *Prahl et al.* [2003]).

[23] Given these constraints on $[19'Hex/K_{37}]_{apc}$ values and the assumption that the responses found in the clone used in our experiments is representative of the alkenone-producing community at Station ALOHA, %Hapto estimates can be made from measured concentrations of 19'Hex and K_{37} in the water column at Station ALOHA. If cells at the depth of maximum alkenone concentration are growing exponentially, they would contribute only ~6-10% and ~2-5% to the total haptophyte community in winter and summer/fall, respectively (Table 1). Waters at the depth of maximum alkenone concentration are chronically nitrate-depleted [*Karl et al.*, 2002, *Letelier et al.*, 2004] however, so one might assume that cells at this depth are in a stationary growth phase. Although our ^{13}C-uptake experiments (see below) indicate that cells at this depth are producing alkenones, it is not possible from our results to determine if they are actually dividing. Assuming the stationary growth value of $[19'Hex/K_{37}]_{apc}$ (i.e., 0.04, Fig. 2C) applies at the depth of the K_{37} concentration maximum, solution of eqn. 3 suggests the contribution of alkenone producing cells to the total haptophyte community is less than ~4% in winter and less than ~2% in summer/fall (Table 1).

[24] 19'Hex concentrations are highly correlated with chlorophyll concentrations at Station ALOHA and consequently maximize in the DCML. On the other hand, K_{37} concentrations at the depth of the DCML are generally quite low throughout the year (Fig. 1). Assuming cells within the DCML are exponentially growing, %Hapto estimates for the DCML are <1-3% in all seasons. The depth of the 1% light level was ~110-120 m from June through August 2001 and ~100-110 m for October 2001 and January-February 2003. However, the DCML persists at a specific potential density surface, yet its depth below the sea-surface can vary up to 50 m on the timescale of hours to days as a result of inertial period and semi-diurnal tidal oscillations [*Karl et al*. 2002]. Consequently, cells at the DCML should experience fluctuating light levels and not constant darkness. Nevertheless, even assigning a $[19'Hex/K_{37}]_{apc}$ value appropriate for cells in continuous darkness (i.e., 0.3, Fig. 2) to yield a maximum %Hapto estimate (~1-8%, Table 1), one still must conclude that alkenone-producing cells contribute negligibly to 19'Hex concentrations at the depth of the DCML.

[25] Our conclusion that alkenone-producing haptophytes contribute so little to the 19'Hex signal anywhere in the euphotic zone at Station ALOHA is potentially not without precedent. Using molecular probes, *Moon-van de Staay et al*. [2000] found that taxa other than haptophytes may have been responsible for the level of 19'Hex observed in waters from the open, oligotrophic subequatorial and equatorial regions of the Pacific.

[26] For purposes of comparison with Station ALOHA, we used the data set of *Shin et al.* [2002] to make %Hapto estimates for surface waters from the Bering Sea during a major *E. huxleyi* bloom in 2000. In those waters, K_{37} concentration ranged from 190-3120 ng L^{-1} and 19'Hex concentration ranged from 30-810 ng L^{-1} at 0-5m depth for the four stations sampled. Assuming cells were growing exponentially under nutrient-replete conditions, %Hapto estimates ranged from a minimum of 7% (Station BR5) to 104% (Station BR 10). However, the concentrations of nitrate + nitrite + ammonium at Station BR 10 was only 0.15 μM and the total C_{37} turnover rate was the lowest measured [*Shin et al*., 2002] suggesting that *E. huxleyi* cells at this site were likely nitrogen-limited and either in a late logarithmic or

stationary growth phase. Assuming a stationary growth value for $[19'Hex/K_{37}]_{apc}$ (~0.04, Fig. 2), %Hapto at Station BR 10 was estimated to be 42%. Despite the range of variability, our calculations show alkenone-producing algae contribute quite significantly to the total haptophyte biomass under *E. huxleyi* bloom conditions This intuitively expected finding for waters experiencing a major *E. huxleyi* bloom suggests that the %Hapto model provides a realistic semi-quantitative sense of how significantly alkenone-producing algae contribute to the haptophyte biomass in given regions.

4.3 Alkenone Production at ALOHA

[27] K_{37} concentration in the water column is conceptually a function of production and loss, one mode of which is export to sediments [*Parsons et al.*, 1984]. Therefore, K_{37} standing stock at any given depth could be low if alkenone losses greatly exceeded production rate or conversely, high if alkenone loss was much lower than its production rate. Consequently, in addition to determining depth profiles for alkenone standing stock in the euphotic zone, we also determined the net alkenone production rates with depth using our *in situ* ^{13}C incubation method. Results showed that production rate was clearly depth-dependent and the depth of maximum alkenone standing stock coincided with that of maximum alkenone production (Fig 1).

[28] We tested assumptions underlying alkenone production rate calculations based on ^{13}C labeling using results from laboratory batch culture experiments (Table 2). Regression analysis of production rates determined using alkenone ^{13}C labeling versus production rates determined from the change in K_{37} concentrations in these experiments yielded a slope and intercept not significantly different ($p < 0.01$) from one and zero, respectively. These results imply that short-term (24 h) incubations provided a reasonable measure of alkenone production rate. *Hamanaka et al.* [2000] and *Shin et al*. [2002] suggested that the $K_{37:2}$ and $K_{37:3}$ production rates could be used to determine the instantaneous $U^{K'}_{37}$ (PR-$U^{K'}_{37}$) or the $U^{K'}_{37}$ set by the cells during the course of the incubation. Although conventional $U^{K'}_{37}$

measurements during our laboratory experiments matched the actual isothermal experimental temperatures well, PR-$U^{K'}_{37}$ consistently yielded overestimates (Table 2). Under isothermal conditions, PR-$U^{K'}_{37}$ would match the culture temperature only if the rates of $K_{37:2}$ and $K_{37:3}$ labeling are identical. In our experiments, the rate of ^{13}C labeling of $K_{37:2}$ consistently exceeded that of $K_{37:3}$ (Table 3), a pattern also displayed in experimental samples from *in situ* incubations conducted in our study at Station ALOHA (data not shown) and in the Bering Sea [*Shin et al.*, 2002]. Based on these findings, we conclude that the proposed ^{13}C-labeling method of assessing instantaneous $U^{K'}_{37}$ values [*Hamanaka et al.*, 2000] is not a realistic prospect. The observed differential labeling rate of the K_{37} compounds is a consequence of the pulse-chase ^{13}C tracer approach and reflects cellular dynamics of the alkenone biosynthetic process. Therefore, we have not calculated PR-$U^{K'}_{37}$ values in our field study. Furthermore, our findings indicate that the ^{13}C labeling method would provide a nearly equivalent but nonetheless not identical assessment of alkenone production rates if calculated using data for $K_{37:2}$ or $K_{37:3}$. Our reported results are based on analysis of data for $K_{37:2}$, the predominant alkenone in samples from Station ALOHA.

[29] Although K_{37} concentration and $K_{37:2}$ production rate maxima occurred at similar depths, highest production rate did not equate with highest standing stock in our seasonal dataset at Station ALOHA (Fig. 1). We measured highest alkenone production rates in summer (KOK-0111), a time when K_{37} concentration was a factor of 2-3 lower than in winter (KOK-0303). The implication of this finding is that measurement of standing stock alone does not allow conclusive interpretation of alkenone production rates or sedimentary export (see also *Prahl et al*. [2005]). On the other hand, surprisingly consistent $K_{37:2}$ turnover rates were observed in the SML throughout the year (Fig. 1C-F). $K_{37:2}$ turnover rates should reflect the physiological state of the alkenone-producing algae. Therefore, these results indicate that cellular alkenone production rates are reasonably uniform throughout the year and that the seasonal change in K_{37} standing stock is controlled mainly by loss. However, it is not possible given available data to determine any more specifically how alkenone loss on

a seasonal basis is apportioned between recycling within the upper water column and sedimentary export, the latter process being of key interest to paleoceanographic studies.

4.4 Alkenone Unsaturation Patterns in the Euphotic Zone

[30] $U^{K'}_{37}$ values recorded in particles from each sampling period (Table 1) were converted into water temperature estimates ($U^{K'}_{37} = 0.034T + 0.039$: *Prahl et al.* [1988]) and plotted versus depth for each season (Figure 3). $U^{K'}_{37}$-estimated temperatures are nearly always different from measured *in situ* temperatures with systematic seasonal differences apparent. $U^{K'}_{37}$-derived temperatures overestimated *in situ* wintertime (KOK-0303) temperatures by ~1.5°C in the SML, where K_{37} concentration and $K_{37:2}$ production rate reach their maximum (Figs. 1C,F and 3C). This overestimate has been ascribed to a change in the haptophyte ecology at ALOHA to alkenone-producing species that exhibit different $U^{K'}_{37}$ responses to growth temperature [*Prahl et al.*, 2005]. In that study, we showed that only a small change in the calibration equation used to calculate growth temperature from $U^{K'}_{37}$ would be required to explain the uniform ~1.5°C overestimate of *in situ* temperatures. On the other hand, $U^{K'}_{37}$-derived temperatures significantly underestimated summer (KOK-0111) and fall (HOT-131) *in situ* temperatures at the depth where $K_{37:2}$ production rates reached their maximum (Fig. 3A, B). Underestimation occurred in the upper 20 m of the thermocline in summer and in the SML in fall. Within the SML in summer (KOK-0111) where production rates are lower than in the upper thermocline, while considerable scatter in $U^{K'}_{37}$ exists, the average $U^{K'}_{37}$-derived temperatures were not significantly (two sample t-test assuming unequal variance, $p = 0.088$, $n = 7$) different from *in situ* temperatures (Fig. 3A, Table 1). Finally, $U^{K'}_{37}$-derived temperatures overestimated *in situ* temperatures at and below the DCML throughout the year. The overestimate of *in situ* DCML temperatures is obvious in summer and fall but is even apparent in the wintertime where the average difference between $U^{K'}_{37}$-derived temperatures and *in situ* temperatures are larger below the SML (2.0±0.3°C) than they are within the SML (1.5±0.1°C; Fig. 3, Table 2).

[31] *Prahl et al.* [2005] suggested that the $U^{K'}_{37}$-derived overestimate of *in situ* temperatures at and below the DCML throughout the year was a physiological response to light limitation on the growth rate of alkenone-producing algae and hence, $K_{37:2}$ production rates (see also *Prahl et al*. [2003]). To further investigate this prospect, we tested experimentally for light limitation on alkenone production rates. We examined $K_{37:2}$ production rate as a function of PAR at the depth of incubation (Fig. 4). At depths greater than ~80 m, PAR is consistently less than ~60 μEin m^{-2} s^{-1} throughout the year and $K_{37:2}$ production rates are correlated with PAR (solid line in Fig. 4). On the other hand, the correlation is improved if the production rate at 50 m (PAR = 131 μEin m^{-2} s^{-1}) measured during KOK-0111 is also included. Saturating light intensities reported for laboratory cultures of *E. huxleyi* range from 72 to >600 μEin m^{-2} s^{-1} for photosynthesis (*Paasche* [1964]: 107 μEin m^{-2} s^{-1}; *Nielsen* [1995]: 72–114 μEin m^{-2} s^{-1}; *Nielsen* [1997]: 117–299 μEin m^{-2} s^{-1} (depending on the acclimation light intensity); *Balch et al*. [1992]: 351–1000 μEin m^{-2} s^{-1} (depending on temperature and nitrate concentration); *Zondervan et al*. [2002]: ~80 μEin m^{-2} s^{-1}). The observed correlation with PAR is consistent with alkenone production being light-limited and is likely responsible for the $U^{K'}_{37}$-derived overestimate of *in situ* temperatures in the DCML. Furthermore, constraint of this correlation to PAR ≤100μEin m^{-2} s^{-1} indicates the lower limit on saturating irradiances defined by results from laboratory culture experiments with *E. huxleyi* is characteristic of that for natural populations at Station ALOHA.

[32] We also investigated light limitation effects on alkenone production rates by collecting water at the DCML on two cruises and incubating it at a shallower depth where PAR was higher. The DCML at Station ALOHA is situated near the nitracline [*Letelier et al.*, 2004] and thus close to an abundant supply of fixed inorganic nitrogen. Our assumption was that relief of light-limitation on cells residing in the nutrient-replete DCML would stimulate $K_{37:2}$ production rate. In all cases, incubating DCML water at a shallower depth stimulated $K_{37:2}$ production rate (Table 4). During KOK-0111, incubating water collected from the DCML (~3 μEin m^{-2} s^{-1}) at 25 m (~490 μEin m^{-2} s^{-1}) increased $K_{37:2}$ production rates by a factor of ~7. During KOK-0303, incubating water from the DCML (~7 μEin m^{-2} s^{-1}) at 100 m (~17

μEin m^{-2} s^{-1}), 80 m (~42 μEin m^{-2} s^{-1}) and 40 m (~245 μEin m^{-2} s^{-1}) increased $K_{37:2}$ production rates by a factor of 2, 14 and 38, respectively. Clearly these results indicate that the physiology of the alkenone-producing cells residing in the DCML was in some way affected by incubations at a shallower depth. Although the increase in $K_{37:2}$ production rates could have been due to the effect of the small increase in temperature (~2.5°C in summer experiment; ≤1°C in winter) on growth rate [*Eppley*, 1972], the results of our depth shift experiments taken in conjunction with the apparent dependence of $K_{37:2}$ production rate on PAR (Fig. 4) strongly suggest that relief of light limitation is the key explanation for the noted increase in $K_{37:2}$ production rates. Since several workers [*Epstein et al.*, 2001; *Versteegh et al*., 2001; *Prahl et al.* 2003] have shown that low light can increase significantly $U^{K'}_{37}$, it follows that the overestimate of $U^{K'}_{37}$-derived temperatures at the DCML throughout the year could be at least partially due to the effects of low light. An alternative hypothesis is that alkenones at the depth of the DCML are in part derived from sinking particles with $U^{K'}_{37}$ values representing growth in warmer, shallower water. We reject this hypothesis based on results from KOK-0111. Highest alkenone production during that cruise occurred just below the SML where $U^{K'}_{37}$-derived temperatures are equal to or lower than the in situ temperature at the DCML. Sinking particles derived from this depth of greatest production would bias $U^{K'}_{37}$ values in the DCML to lower, not higher temperatures.

[33] If our interpretation of the effect of light limitation on the physiology of alkenone producing algae residing in the DCML is correct, it follows that growth under the extreme nutrient limitation characteristic of Station ALOHA at the depth of the alkenone production maximum may have affected the $U^{K'}_{37}$ of cells at depths where light was not limited. Phytoplankton growth in the upper region (0–90 m) of the euphotic zone at Station ALOHA is thought to be almost permanently under nutrient-limiting conditions [e.g., *Letelier et al*., 2004]. The historic nitrate and phosphate levels at this site are consistent with nutrient-limitation on the growth of the alkenone-producing algae (see web archive for HOT program referenced above). $U^{K'}_{37}$ temperatures underestimated measured temperatures at the depth of the $K_{37:2}$ production maximum by 1.8-2.3°C in the summer and 2.3-2.9°C in the fall (Fig. 3,

Table 2). Several authors [*Epstein et al.*, 1998; *Versteegh et al*., 2001; *Prahl et al.* 2003] have shown that growth of alkenone-producing haptophytes under nutrient limitation can alter values of $U^{K'}_{37}$ by amounts equivalent to a 2-3°C change in growth temperature. Assuming these experimental findings for laboratory cultures apply to natural populations, the underestimate of *in situ* temperature could reflect the communities' physiological response to the highly limited availability of nutrients at these depths. Although inclusion of the production rate measurement at 50 m during KOK-0111 improved the correlation between $K_{37:2}$ production rate and PAR (dashed line, Fig. 4) suggesting light limitation on $K_{37:2}$ production rate even at 50 m, the underestimate of $U^{K'}_{37}$ throughout the thermocline in summer is consistent with the effects of nutrient limitation. The 50 m datum may fall in the transition between first-order and zero-order kinetic control of light on production rate and therefore the improved correlation was simply fortuitous.

[34] Despite the complexities in alkenone biogeochemistry, $U^{K'}_{37}$ and CTD temperature for all water column samples at Station ALOHA plot within ±3°C of the global ocean $U^{K'}_{37}$ – maSST calibration equation now established by *Muller et al.* [1998] from analysis of core top sediments (Fig. 5). It should also be kept in mind that our sediment trap study at Station ALOHA [*Prahl et al.*, 2005] showed that the $U^{K'}_{37}$ temperature estimates derived from the flux-weighted average $U^{K'}_{37}$ estimated temperatures were only slightly warmer than maSST during 1992-1993 and essentially the same in 2000-2001. Therefore, while our Station ALOHA studies strongly suggest that the genetic and non-thermal physiological factors identified previously in laboratory experiments can be apparent in water column field data, the average $U^{K'}_{37}$ value transmitted to the paleo-record at this site still provide a reasonable estimate of mean annual sea-surface temperature.

5. Conclusions and Implications

[35] Our seasonal study at Station ALOHA indicated that the alkenone producing algae were a small fraction of the haptophyte community and implied that their ecology differed

significantly from that of the major phytoplankton species contributing to the 19'Hex distribution at this site. Results showed that the $K_{37:2}$ production rate was depth-dependent and that the depth of maximum K_{37} standing stocks and $K_{37:2}$ production rates are essentially coincident. Nevertheless, we found significant seasonal variations in K_{37} concentrations. Since $K_{37:2}$ turnover rates were reasonably constant throughout the year, our results imply that alkenone loss controlled the seasonal change in K_{37} concentrations and indicate that K_{37} standing stock measurements alone do not allow conclusive interpretation of alkenone production and loss either via *in situ* recycling or export to sediments.

[36] We found that $U^{K'}_{37}$-estimated and measured *in situ* temperatures are nearly always different with systematic seasonal differences quite apparent. We propose that this discrepancy is explained by ecological and now recognized non-thermal physiological effects on $U^{K'}_{37}$. A change in ecology at Station ALOHA to a dominance of alkenone-producing haptophytes that display a $U^{K'}_{37}$ response to growth temperature slightly different from the commonly used calibration is perhaps the most straightforward explanation for the uniform ~1.5°C overestimate of *in situ* temperatures throughout the SML during wintertime. On the other hand, non-thermal physiological factors best account for discrepancies in measured and estimated temperatures noted above during summer and fall as well as at the DCML throughout the year. In the DCML where production rates were always lowest, the lack of light apparently affected the physiology of alkenone-producing algae such that the $U^{K'}_{37}$-estimated growth temperature overestimated actual water temperature by ~2-4ºC. In the fall and summer when production rates were high in or just below the SML, the 2-3ºC $U^{K'}_{37}$ underestimate of actual water temperature probably reflected the communities' physiological response to the highly limited availability of nutrients at these depths.

[37] Using predictions of alkenone export depth derived from $U^{K'}_{37}$ measurements in a recent study of sediment trap time series from 2800 m at Station ALOHA, *Prahl et al*. [2005] showed that alkenone export events were synchronized with the seasonal pattern for total export production and appear controlled by two fundamentally different processes during the

year: export production from N_2 fixation which is greatest when surface waters are most highly stratified (June to August), and more traditional, nitrate-supported export production which maximizes in winter (February to March) when surface mixing penetrates deepest. Our present study also indicated that the observed wintertime overestimate of $U^{K'}_{37}$-derived temperatures in the SML was consistent with inferences from the wintertime alkenone signal recorded in both a 1992-93 and 2000-01 sediment trap time series. On the other hand, the depth of alkenone export estimated from $U^{K'}_{37}$ measurements in the sediment trap time series matched well the depth of subsurface oxygen supersaturation throughout summer [*Prahl et al.*, 2005]. During our summer cruise, the K_{37} concentrations and $K_{37:2}$ production rates were indeed maximized within the depth zone of oxygen supersaturation.

[38] From the paleoceanographic viewpoint, it is important to emphasize that for Station ALOHA both the $U^{K'}_{37}$ temperature estimates derived from the flux-weighted average $U^{K'}_{37}$ from the sediment trap time series [*Prahl et al.*, 2005] and the $U^{K'}_{37}$-CTD temperature relationship for the water column samples fall within the apparent scatter of the global calibration for $U^{K'}_{37}$ versus maSST [*Muller et al*., 1998]. Therefore, the average $U^{K'}_{37}$ value transmitted to the paleo-record at this site still provide a reasonable mean annual sea-surface temperature estimate even though results from our study of living alkenone-producers in surface waters at Station ALOHA strongly suggest that the genetic and non-thermal physiological factors previously identified in laboratory culture experiments are well-expressed in natural waters at Station ALOHA and potentially many others sites.

Acknowledgements – We wish to thank: David M. Karl, John E. Dore and the JGOFS HOT Program personnel for accommodation on HOT-131 and for access to ancillary oceanographic data from Station ALOHA; Francis J. Sansone (chief scientist on KOK-0111) who allowed us ample time in the middle of the night for our experiments and sample collection; Donielle Chittenden, Bryan Deschenes, Denby Fern, Terri Rust, Margaret Sparrow, Katsumasa Tanaka and Dana Vukajlovich for assistance in the laboratory and on the cruises; and Dave Gravatt and the Captains and crew of the *R/V Kaimikai-o-Kanaloa* for

facilitating our field work at Station ALOHA. This research was supported by National Science Foundation grants OCE-0094272 (BNP), OCE-9986306 and OCE-0094329 (FGP), OCE-9986306 and OCE-0094637 (BNP, R.R. Bidigare and E.A. Laws). This is SOEST contribution number ####.

6. References

Balch W. M., P. M. Holligan, and K. A. Kilpatrick (1992) Calcification, photosynthesis and growth of the bloom forming coccolithophore, *Emiliania huxleyi*, *Cont. Shelf Res. 12*, 1353–1374.

Brassell S. C. (1993), Applications of biomarkers for delineating marine paleoclimatic fluctuations during the Pleistocene, In *Organic Geochemistry: Principles and Applications* (eds. M. H. Engel and S. A. Macko), pp. 699-738. Plenum Press.

Brassell S. C., G. Eglinton, I. T. Marlowe, U. Pflaumann and M. Sarnthein (1986), Molecular stratigraphy: a new tool for climatic assessment, *Nature 320*, 129-133.

Brock T. D. (1981) Calculating solar radiation for ecological studies, *Ecol. Modell. 14***,** 1–19.

Conte M. H., A. Thompson, D. Lesley and R. Harris (1998), Genetic and physiological influences on the alkenone/alkenoate versus growth temperature relationship in *Emiliania huxleyi* and *Gephyrocapsa oceanica*. *Geochim. Cosmochim. Acta 62*, 51-68.

Christie W. W. (1973), *Lipid Analysis: Isolation, Separation, Identification and Structural Analysis of Lipids*. Pergamon Press.

Cortes M. Y., J. Bollmann and H. R. Thierstein (2001), Coccolithophore ecology at the HOT station ALOHA, Hawaii, *Deep-sea Research II 48*, 1957-1981.

Deines P., D. Langmuir and R. S. Harmon (1974), Stable carbon isotope ratios and the existence of a gas phase in the evolution of carbonate ground waters, *Geochim. Comochim. Acta 38*, 1147-1164.

Dickson A. G. (1990a), Standard potential of the reaction: AgCL(s) + 1.2H_2(g) = Ag(s) + 11Cl(aq), and the standard acidity constant of the ion HSO_4^- in synthetic seawater from 273.15 to 318.15°K, *J. Chem. Thermodyn. 22*, 113-127.

Dickson A. G. (1990b), Thermodynamics of the dissociation of boric acid in synthetic seawater 273.15 to 318.15°K, *Deep-Sea Res., Part A 37*, 755-766.

Duffie J. A. and W. A. Beckman (1980) Solar engineering of thermal processes, 2nd Edition, Wiley, 919 p.

Eppley R. W. (1972), Temperature and phytoplankton growth in the sea, *Fish Bulletin 70*, 1063-1085.

Epstein B. L., S. d'Hondt, J. G. Quinn, J. Zhang and P. E. Hargraves (1998), An effect of dissolved nutrient concentrations on alkenone-based temperature estimates, *Paleocean. 13*, 122-126.

Epstein B. L., S. d'Hondt and P. E. Hargraves (2001), The possible metabolic role of C37 alkenones in *Emiliania huxleyi*, *Org. Geochem. 32*, 867-875.

Green J. C. and B. S. C. Leadbetter (1994), *The Haptophyte Algae*. Claredon Press.

Hama T., J. Hama and N. Handa (1993) ^{13}C tracer methodology in microbial ecology with special reference to primary production processes in aquatic environments. In *Advances in Microbial Ecology* (ed. J. GWYNFRYN), pp. 39-83. Plenum Press

Hamanaka J., K. Sawada and E. Tanoue (2000), Production rates of C_{37} alkenones determined by ^{13}C-labeling technique in the euphotic zone of Sagami Bay, Japan, *Organic Geochemistry 31*, 1095-1102.

Hayes J. M., K. H. Freeman, B. N. Popp and C. H. Hoham (1990), Compound-specific isotopic analyses: a novel tool for reconstruction of ancient biogeochemical processes, *Organic Geochemistry 16*, 1115-1128.

Jeffrey S. W., R. F. C. Mantoura and S. W. Wright (1997), *Phytoplankton pigments in oceanography*, UNESCO Publishing.

Johnson K. M., K. D. Willis, W. K. Butler, W. K. Johnson, and C. S. Wong (1993) Coulometric total carbon dioxide analysis for marine studies: Maximizing the performance of an automated gas extraction system and coulometric detector, *Marine Chemistry 44,* 167-188.

Karl, D. M., and R. Lukas (1996), The Hawaii Ocean Time-series (HOT) Program: Background rationale and field implementation, *Deep Sea Res. 43*, 129–156.

Karl D. M., R. R. Bidigare and R. M. Letelier (2002), Chapter 9: Sustained and aperiodic variability in organic matter production and phototrophic microbial community structure in the North Pacific subtropical gyre. In *Phytoplankton Productivity: Carbon Assimilation in Marine and Freshwater Ecosystems* (ed. P. J. l. Williams, D. N. Thomas, and C. S. Reynolds), pp. 222-264. Blackwell Science Ltd.

Kroopnick P. (1985), The distribution of ^{13}C in ΣCO_2 in the world oceans, *Deep-sea Research I 32*, 57-84.

Laws E. A., B. N. Popp, R. R. Bidigare, M. C. Kennicutt and S. A. Macko (1995), Dependence of phytoplankton carbon isotopic composition on growth rate and $[CO_2]_{aq}$: theoretical considerations and experimental results, *Geochimica et Cosmochimica Acta 59*, 1131-1138.

Laws E. A., B. N. Popp, R. R. Bidigare, U. Riebesell, S. Burkhardt and S. G. Wakeham (2000) Controls on the molecular distribution and carbon isotopic composition of alkenones in certain haptophyte algae, *Geochemistry, Geophysics, and Geosystems*, *2*, Paper number 2000GC000057.

Letelier R. M., R. R. Bidigare, D. V. Hebel, M. Ondrusek, C. D. Winn and D. M. Karl (1993), Temporal variability of phytoplankton community structure based on pigment analysis, *Limnol. Oceanogr. 38*, 1420-1437.

Letelier R. M., D. M. Karl, M. R. Abbott and R. R. Bidigare (2004), Light driven seasonal patterns of chlorophyll and nitrate in the lower euphotic zone of the North Pacific Subtropical Gyre, *Limnology and Oceanography 49*, 508-519.

Lewis E. and D. W. R. Wallace (1998) Program Developed for CO_2 System Calculations. ORNL/CDIAC-105. Carbon Dioxide Information Analysis Center, Oak Ridge National Laboratory, U.S. Department of Energy, Oak Ridge, Tennessee.

Longhurst A. R. and W. G. Harrison (1989) The biological pump: Profiles of plankton production and consumption in the upper ocean, *Progress in Oceanography 22,* 47-123.

Marlowe, I. T., J. C. Green, A. C. Neal, S. C. Brassell, G. Eglinton, and P. A. (1984), Course, Long-chain (C_{37} -C_{39}) alkenones in the Prymnesiophyceae. Distribution of alkenones and other lipids and their taxonomic significance, *Br. Phycol. J. 19*, 203-216.

Marlowe, I. T., S. C. Brassell, G. Eglinton, and J. C. Green (1990), Long-chain alkenones and alkyl alkenoates and the fossil coccolith record of marine sediments, *Chem. Geol. 88*, 349-375.

Millero F. J. (1979), The thermodynamics of the carbonic acid system in seawater, *Geochim. Cosmochim. Acta*, *43*, 1651-1661.

Mook W. G., J. C. Bommerson and W. H. Staberman (1974), Carbon isotope fractionation between dissolved bicarbonate and gaseous carbon dioxide, *Earth Planet Sci. Lett. 22*, 169-176.

Moon-van der Staay S.Y., G. W. M. van der Staay, L. Guillou, D. Vaulot, H. Claustre and L. K. Medlin (2000), Abundance and diversity of prymnesiophytes in the picoplankton community from the equatorial Pacific Ocean inferred from 18S rDNA sequences, *Limnol. Oceanogr. 45*, 98-109.

Muller P. J., G. Kirst, G. Ruhland, I. von Storch and A. Rosell-Mele (1998), Calibration of the alkenone paleotemperature index $U^{K'}_{37}$ based on core-tops from the eastern South Atlantic and the global ocean (60^{o}N-60^{o}S), *Geochim. Cosmochim. Acta 62*, 1757-1772.

Nielsen M. V. (1995) Photosynthetic characteristics of the coccolithophorid *Emiliania huxleyi* (Prymnesiophyceae) exposed to elevated concentrations of dissolved inorganic carbon, *J. Phycol*. *31*, 715-719.

Nielsen M.V., 1997. Growth, dark respiration and photosynthetic parameters of the coccolithophorid *Emiliania huxleyi* (Prymnesiophyceae) acclimated to different day length-irradiance combinations, *J. Phycol. 33*, 818-822.

Ohkouchi N., T. I. Eglinton, L. D. Keigwin and J. M. Hayes (2002), Spatial and temporal offsets between proxy records in a sediment drift, *Science 298*, 1224-1227.

Paasche E. (1964) A tracer study of the inorganic carbon uptake during coccolith formation and photosynthesis in the coccolithophorid *Coccolithus huxleyi*, *Physiol. Plant., Suppl. 3*, 1-82.

Pagani M., M. A. Arthur and K. H. Freeman (1999), Miocene evolution of atmospheric carbon dioxide, *Paleoceanography 14*, 273-292.

Pagani M., K. H. Freeman, N. Ohkouchi and K. Caldeira (2002), Comparison of water column $[CO_2]_{aq}$ with sedimentary alkenone-based estimates: a test of the alkenone-CO_2 proxy., *Paleoceanography 17*, 1069, doi: 10.1029/2002PA000756.

Parsons T. R., M. Takahashi and B. Hargrave (1984), *Biological Oceanographic Processe*, Pergamon Press.

Pond W. D. and R. P. Harris (1996), Lipid composition of the coccolithorphore *Emiliania huxleyi* and its possible ecophysiological significance, *J. Mar. Biol. Assoc. U. K. 76*, 579–594.

Popp B. N., F. Kenig, S. G. Wakeham, E. A. Laws and R. R. Bidigare (1998) Does growth rate affect ketone unsaturation and intracellular carbon isotopic variability in *Emiliania huxleyi*? *Paleoceanography 13*, 35-41.

Prahl F. G. and S. G. Wakeham (1987), Calibration of unsaturation patterns in long-chain ketone compositions for palaeotemperature assessment, *Nature 330*, 367-369.

Prahl F. G., L. A. Muehlhausen and D. L. Zahnle (1988), Further evaluation of long-chain alkenones as indicators of paleoceanographic conditions, *Geochim. Cosmochim. Acta 52*, 2303-2310.

Prahl F. G., L. A. Muehlhausen and M. Lyle (1989), An organic geochemical assessment of oceanographic conditions at MANOP Site C over the past 26,000 years, *Paleoceanography 4*, 495-510.

Prahl F. G., T. Herbert, S. C. Brassell, N. Ohkouchi, M. Pagani, D. Repeta, A. Rosell-Mele and E. Sikes (2000), Status of alkenone paleothermometer calibration: report from Working Group 3, *Geochemistry, Geophysics and Geosystems 1*, 1-13.

Prahl F. G., G. V. Wolfe and M. A. Sparrow (2003), Physiological impacts on alkenone paleothermometry, *Paleoceanography 18*, 1025, 2002PA000803.

Prahl F. G., B. N. Popp, D. M. Karl and M. A. Sparrow (2005), Ecology and biogeochemistry of alkenone production at Station ALOHA, *Deep-Sea Res. I* 52, 699-719.

Rost B., U. Riebesell, S. Burkhardt and D. Sültemeyer (2003) Carbon acquisition of bloom-forming marine phytoplankton, *Limnol. Oceanogr.*, 48, 55-67.

Roy R. N., L. N. Roy, K. M. Vogel, C. P. Moore, T. Pearson, C. E. Good, F. J. Millero and D. M. Cambell (1993), Determination of the ionization constants of carbonic acid in seawater, *Mar. Chem 44*, 249-268.

Shin K.-H., N. Tanaka, N. Harada and J.-C.Marty (2002), Production and turnover rates of C_{37} alkenones in the eastern Bering Sea: implication for the mechanism of a long duration of *Emiliania huxleyi* bloom, *Progress in Oceanography 55*, 113-129.

Strickland J. D. H. and T. R. Parsons (1972), *A Practical Handbook of Seawater Analysis*, Second Edition ed., Vol. Bulletin 167, Fisheries Research Board of Canada, 310p.

Van Lenning, K. I. Probert, M. Latasa, M. Estrada and J. R. Young (2004) Pigment diversity of coccolithophores in relation to taxonomy, phylogeny and ecological preferences In: Thierstein, H. and Young, J. (Eds.) Coccolithophores: From Molecular Processes to Global Impact, Springer Verlag: pp 51-73.

Versteegh, G.J.M., R. Riegman, J. W. deLeeuw, and J. H. F. Jansen (2001), $U^{K'}_{37}$ values for *Isochysis galbana* as a function of culture temperature, light intensity and nutrient concentrations, *Org. Geochem. 32*, 785-794.

Volkman, J. K., S. M. Barrett, S. I. Blackburn, and E. L. Sikes (1995), Alkenones in *Gephyrocapsa oceanica*: Implication for studies of paleoclimate, *Geochim. Cosmochim. Acta 59*, 513-520.

Zondervan I., B. Rost and U. Riebesell (2002) Effect of CO_2 concentration on the PIC/POC ratio in the coccolithophore *Emiliania huxleyi* grown under light-limiting conditions and different daylengths, *Jour. Exp. Mar. Biol. Ecol. 272*, 55-70.

7. Figure Captions

Figure 1. Profiles for K_{37} concentration (filled circles), $K_{37:2}$ production rate (filled squares) and $K_{37:2}$ turnover rate (open circles) with depth throughout the euphotic zone at Station ALOHA for KOK 0111 in July 2001 (A, D), HOT 131 in October 2001 (B, D) and KOK 0303 in February 2003 (C, E). For reference purposes, plots A-C have been annotated with the profiles for temperature (dashed line) and chlorophyll *a* concentration (solid line) measured using the *in situ* CTD package and fluorometer, respectively, attached to the water sampling package and plots D-F for PAR (solid line, see text for details).

Figure 2. Batch culture experiments conducted with *E. huxleyi* (CCMP 1742) to test the effect of (A, C) nutrient depletion (Nutrient Stress Experiment) and (B, D) darkness (Darkness Stress Experiment) on cellular pigment and alkenone contents. The shaded areas in plots B and D indicate a 5-day period in the light limitation experiment when the culture flask was covered with sufficient aluminum foil to exclude all light but not to impede gaseous exchange between the culture media and the atmosphere. Plots A and B display growth curves for each experiment. Lines identify the portion of each curve used to calculate exponential growth rates (0.37-0.40 d^{-1}). Data showing drawdown of nitrate and phosphate concentration in each experiment are also plotted.

Figure 3. Profiles for $U^{K'}_{37}$-estimated water temperatures (filled circles) with depth throughout the euphotic zone at Station ALOHA in (A) summer (KOK 0111, July 2001), (B) fall (HOT 131, October 2001) and (C) winter (KOK 0303, February 2003). $U^{K'}_{37}$ temperatures were estimated using the calibration of *Prahl et al.* [1988] (see text for details). For reference purposes, these plots have been annotated with the profiles for temperature (dashed line) and chlorophyll *a* concentration (solid line) measured using the *in situ* CTD package and fluorometer, respectively, attached to the water sampling package.

Figure 4. Plot of the photosynthetic active radiation (PAR) as a function of the $K_{37:2}$ production rate at Station ALOHA. The shaded box represents the approximate lower limits on saturating irradiances for *E. huxleyi* based on culture experiments (see text for details). The solid line in the plot represents a linear least-squares regression analysis fit to the data with PAR <~80 μEin m^{-2} s^{-1} from all three cruises ($y = 0.007x + 0.04$, $r^2 = 0.64$). The dashed line in the plot represents a linear least-squares regression analysis fit to the data with PAR <130 μEin m^{-2} s^{-1} from all three cruises ($y = 0.011x - 0.02$, $r^2 = 0.95$).

Figure 5. Plot of $U^{K'}_{37}$ as a function of CTD temperature for all water column samples measured (KOK 0111 - July 2001, HOT 131 - October 2001, KOK 0303 - February 2003). The solid line in the plot represents the $U^{K'}_{37}$ correlation with mean annual sea surface

temperature from global ocean core top sediments of *Muller et al.* [1998] whereas the dashed lines represent a ±3°C window of uncertainty surrounding the calibration line.

Table 1. K_{37} concentrations, cell density calculated from K_{37} concentration (see text for details), %Hapto estimates (see eqn. 3 and text for details) and alkenone unsaturation patterns ($U^{K'}_{37}$) determined from analysis of surface waters at Station ALOHA. ΔT is defined as the difference between estimated ($U^{K'}_{37}$-T) and measured (CTD-T) temperature, where $U^{K'}_{37}$-T is calculated from $U^{K'}_{37}$ using the calibration equation of *Prahl et al.* [1988].

Cruise/Samples	Depth, m	Depth Zone	[K_{37}], ng L^{-1}	Density, cell L^{-1}	%Hapto	$U^{K'}_{37}$	CTD-T, °C	ΔT, °C
KOK-0111, July 2001								
Shipboard Pump	7	SML	3.0	4.0×10^3	2.7 (1.1)[a]	0.911	25.3	0.3
Shipboard Pump	7	SML	3.2	4.3×10^3	2.9 (1.2)[a]	0.846	25.3	-1.6
Shipboard Pump	7	SML	2.3	3.1×10^3	2.1 (0.8)[a]	0.904	25.3	0.1
Shipboard Pump	7	SML	4.0	5.3×10^3	3.6 (1.5)[a]	0.836	25.3	-1.9
Shipboard Pump	7	SML	2.3	3.1×10^3	2.1 (0.8)[a]	0.864	25.3	-1.0
In Situ Pump	20	SML	2.6	3.5×10^3	2.4 (0.9)[a]	0.901	25.3	0.0
CTD Rosette	25	SML	1.6	2.1×10^3	1.5 (0.6)[a]	0.911	25.3	0.3
In Situ Pump	49	Thermocline	5.5	7.3×10^3	2.4 (1.0)[a]	0.795	24.8	-2.5
In Situ Pump	50	Thermocline	5.3	7.1×10^3	1.8 (0.7)[a]	0.809	24.7	-2.0
In Situ Pump	50	Thermocline	4.5	6.0×10^3	1.5 (0.6)[a]	0.812	24.7	-1.9
CTD Rosette	50	Thermocline	5.7	7.6×10^3	1.9 (0.8)[a]	0.808	24.7	-2.0
In Situ Pump	53	Thermocline	5.5	7.3×10^3	1.8 (0.7)[a]	0.788	24.4	-2.3
In Situ Pump	55	Thermocline	4.9	6.5×10^3	1.6 (0.7)[a]	0.800	24.2	-1.8
In Situ Pump	63	Thermocline	5.5	7.3×10^3	1.8 (0.7)[a]	0.766	23.9	-2.5
In Situ Pump	65	Thermocline	5.8	7.7×10^3	1.9 (0.8)[a]	0.756	23.9	-2.8
In Situ Pump	70	Thermocline	6.7	8.9×10^3	1.5 (0.6)[a]	0.753	23.8	-2.8
CTD Rosette	80	Thermocline	4.5	6.0×10^3	1.0 (0.4)[a]	0.762	23.2	-2.0
In Situ Pump	96	DCML	3.7	4.9×10^3	0.7 (2.2)[b]	0.883	22.6	2.3
CTD Rosette	100	DCML	1.8	2.4×10^3	0.3 (0.9)[b]	0.871	22.5	1.9
CTD Rosette	120	DCML	1.2	1.6×10^3	0.2 (0.5)[b]	0.913	22.0	3.7
CTD Rosette	135	DCML	0.8	1.1×10^3	0.1 (0.3)[b]	0.894	21.3	3.8
CTD Rosette	165	DCML	3.0	0.7×10^3	0.2 (0.5)[b]	0.850	20.2	3.7
HOT-131, October 2001								
Shipboard Pump	7	SML	4.9	6.5×10^3	4.5 (1.8)[a]	0.825	25.4	-2.3
In Situ Pump	30	SML	5.0	6.6×10^3	3.7 (1.5)[a]	0.804	25.4	-2.9
In Situ Pump	60	SML	4.8	6.4×10^3	1.7 (0.7)[a]	0.823	25.4	-2.3
CTD Rosette	80	DCML	1.2	1.6×10^3	0.2 (0.7)[b]	0.884	22.1	2.8
In Situ Pump	82	DCML	3.8	5.0×10^3	0.8 (2.3)[b]	0.882	22.0	2.8
In Situ Pump	92	DCML	2.3	3.0×10^3	0.7 (2.2)[b]	0.897	21.7	3.5
In Situ Pump	102	DCML	1.2	1.6×10^3	0.4 (1.1)[b]	0.898	21.3	4.0
CTD Rosette	120	DCML	0.5	0.7×10^3	0.1 (0.4)[b]	0.792	20.6	2.5
KOK-0303, February 2003								
Shipboard Pump	7	SML	9.3	12.4×10^3	7.6 (3.1)[a]	0.886	22.9	2.0
Shipboard Pump	7	SML	8.8	11.7×10^3	7.2 (2.9)[a]	0.876	22.9	1.7
Shipboard Pump	7	SML	12.1	16.2×10^3	9.9 (4.0)[a]	0.875	22.9	1.7
Shipboard Pump	7	SML	12.5	16.6×10^3	10.2 (4.1)[a]	0.866	22.9	1.4
In Situ Pump	17	SML	11.6	15.5×10^3	9.5 (3.8)[a]	0.861	22.9	1.3
In Situ Pump	37	SML	11.7	15.6×10^3	9.6 (3.8)[a]	0.854	22.9	1.1
CTD Rosette	40	SML	9.0	12.0×10^3	7.4 (3.0)[a]	0.898	22.9	2.3
In Situ Pump	57	SML	12.9	17.3×10^3	9.1 (3.6)[a]	0.874	22.9	1.7
In Situ Pump	72	SML	12.4	16.5×10^3	8.0 (3.2)[a]	0.855	22.9	1.1
In Situ Pump	77	SML	11.8	15.7×10^3	7.6 (3.0)[a]	0.879	22.9	1.8
CTD Rosette	80	SML	8.8	11.8×10^3	5.7 (2.3)[a]	0.875	22.9	1.7
In Situ Pump	80	SML	15.5	20.6×10^3	10.0 (4.0)[a]	0.859	22.9	1.2
In Situ Pump	97	DCML	8.3	11.1×10^3	2.7 (8.0)[b]	0.861	22.9	1.3
CTD Rosette	100	DCML	4.0	5.3×10^3	1.3 (3.8)[b]	0.875	22.9	1.7
In Situ Pump	100	DCML	2.5	3.4×10^3	0.8 (2.4)[b]	0.853	22.9	1.0
In Situ Pump	117	DCML	6.8	9.1×10^3	1.3 (4.0)[b]	0.855	22.5	1.5
In Situ Pump	117	DCML	9.5	12.6×10^3	1.8 (5.5)[b]	0.862	22.5	1.7
CTD Rosette	120	DCML	2.7	3.7×10^3	0.5 (1.6)[b]	0.896	22.1	3.1
In Situ Pump	120	DCML	4.9	6.5×10^3	0.9 (2.8)[b]	0.877	22.7	2.5
In Situ Pump	133	DCML	2.7	3.6×10^3	0.5 (1.6)[b]	0.819	22.2	1.2
In Situ Pump	137	DCML	1.4	1.9×10^3	0.3 (0.8)[b]	0.836	21.5	1.8
In Situ Pump	140	DCML	2.6	3.5×10^3	0.8 (2.5)[b]	0.867	22.2	2.7
In Situ Pump	153	DCML	2.9	3.9×10^3	0.9 (2.8)[b]	0.798	21.6	1.1

[a] $[19'\text{Hex}/K_{37}]_{apc} = 0.04$ assumed to be appropriate for nutrient limitation

[b] $[19'\text{Hex}/K_{37}]_{apc} = 0.3$ assumed to be appropriate for light limitation

Table 2. Summary of Measured Variables in Batch Culture Experiments to Investigate the ^{13}C Labeling of Alkenones.

μ, d^{-1}	t, d	ΣCO_2, μmol kg^{-1}	Alkalinity μeq kg^{-1}	δ_{DIC} ‰	$[CO_2(aq)]$ μmol kg^{-1}	δ_{CO_2} ‰	$K_{37:2}$ μg L^{-1}	$U^{K'}_{37}$	$U^{K'}_{37}$ T °C	$\delta_{37:2}$ ‰	$\delta_{37:3}$ ‰	$K_{37:2}$ PR μg L^{-1} d^{-1}	$K_{37:3}$ PR μg L^{-1} d^{-1}	PR-$U^{K'}_{37}$	PR-$U^{K'}_{37}$ T °C
***E. huxleyi* (CCMP 1742), Temperature = 15.3°C**															
0.32	0.00	1.77	2.29	209.4	4.1	198.3	14.3	0.569	15.6	-36.1	-34.1				
0.32	0.50	1.77	2.29	209.4	4.1	198.3	22.4	0.566	15.5	-0.7	-5.6	6.9	4.3	0.615	17.0
0.32	1.00	1.77	2.29	209.4	4.1	198.3	27.1	0.556	15.2	29.9	20.7	7.8	5.2	0.599	16.5
0.32	0.00	1.73	2.28	239.6	3.7	228.2	15.8	0.553	15.1	-36.2	-33.4				
0.32	0.50	1.73	2.28	239.6	3.7	228.2	22.9	0.547	14.9	2.5	-1.5	6.8	4.7	0.592	16.3
0.32	1.00	1.73	2.28	239.6	3.7	228.2	26.6	0.566	15.5	38.4	27.3	7.6	4.8	0.614	16.9
***E. huxleyi* (CCMP 1742), Temperature = 19.5°C**															
0.47	0.00	1.83	2.29	125.9	6.2	116.0	19.1	0.724	20.1	-33.1	-33.8				
0.47	0.50	1.83	2.29	125.9	6.2	116.0	22.7	0.731	20.4	-3.7	-11.2	9.3	8.6	0.781	21.8
0.47	1.00	1.83	2.29	125.9	6.2	116.0	34.6	0.724	20.2	22.4	-9.2	13.0	13.2	0.770	21.5
0.47	2.00	1.83	2.29	125.9	6.2	116.0	62.2	0.725	20.2	52.4	-40.3	18.3	23.6	0.753	21.0
0.47	0.00	1.84	2.30	126.0	6.3	116.1	17.2	0.725	20.2	-18.1	-20.6				
0.47	0.50	1.84	2.30	126.0	6.3	116.1	24.3	0.723	20.1	-0.7	-8.7	6.5	9.4	0.795	22.2
0.47	1.00	1.84	2.30	126.0	6.3	116.1	32.4	0.721	20.1	21.6	10.2	9.9	12.5	0.773	21.6
0.47	2.00	1.84	2.30	126.0	6.3	116.1	50.1	0.731	20.3	47.8	36.1	12.7	18.5	0.763	21.3

Table 3. Total C_{37} alkenone concentrations (K_{37}), $U^{K'}_{37}$-derived water temperature estimates ($U^{K'}_{37}$-T, see text for details), stable carbon isotopic ($\delta^{13}C$) composition of the di-unsaturated C_{37} alkenone ($K_{37:2}$) determined from analysis of natural and ^{13}C-incubated waters at Station ALOHA in three different seasons: summer (KOK-0111, July 2001, fall (HOT-131, October 2001) and winter (KOK-0303, February 2003), calculated K_{37} production and turnover rates. Stdev (n) represents the standard deviation of the $\delta^{13}C$ measurement on $K_{37:2}$ and the number of injections for the sample (n) on the irmGCMS.

Sample Type / *Collection Method*	Collection Depth, m	Incubation Depth, m	K_{37}, ng L^{-1}	$U^{K'}_{37}$-T, ^{o}C	$\delta^{13}C_{37:2}$, ‰ vs. VPDB	Stdev (n)	$K_{37:2}$-PR, ng L^{-1} d^{-1}	Turnover, d^{-1}
KOK-0111: Natural								
Shipboard Pump	7		4.0	23.4	-26.5	±0.3 (3)		
Shipboard Pump	7		2.3	24.3	-26.3	±0.0 (2)		
In Situ Pump	53		5.5	22.1	-27.1	±0.2 (2)		
In Situ Pump	63		5.5	21.4	-26.2	±0.1 (3)		
In Situ Pump	65		5.8	21.1	-25.8	±1.2 (3)		
In Situ Pump	96		3.7	24.9	-27.3	±0.2 (2)		
KOK-0111: *In Situ* ^{13}C-Incubations								
Free-floating Array	25	25	1.6	25.6	6.5	±0.5 (2)	0.22	0.14
Free-floating Array	50	50	5.7	22.7	46.7	±0.1 (2)	1.50	0.37
Free-floating Array	120	120	1.2	25.7	-12.3	(1)	0.07	0.06
KOK-0111: *In Situ* ^{13}C-Incubations (Depth Shift Experiments)								
Free-floating Array	135	25	1.1	24.0	43.8	(1)	0.48	0.44
HOT-131: Natural								
Shipboard Pump	7		4.9	23.1	-25.2	±0.7 (3)		
In Situ Pump	30		5.0	22.5	-23.1	±0.7 (2)		
In Situ Pump	60		4.8	23.1	-23.1	±0.2 (2)		
In Situ Pump	82		3.8	24.8	-24.5	±0.7 (3)		
In Situ Pump	92		2.3	25.2	-23.9	±0.3 (2)		
In Situ Pump	102		1.2	25.3	-19.8	±1.5 (2)		
HOT-131: *In situ* ^{13}C-Incubations								
Free-floating Array	30-60	30-60	3.4	22.8	12.7	±1.8 (3)	0.45	0.13
Free-floating Array	80	80	1.2	24.9	19.3	(1)	0.21	0.18
Free-floating Array	120	120	0.5	23.1	-1.4	(1)	0.04	0.08
KOK-0303: Natural								
Shipboard Pump	7		9.3	24.9	-27.0	(1)		

In Situ Pump	37		11.7	24.0	-27.3	±0.3 (4)		
In Situ Pump	80		15.5	24.1	-26.4	±0.1 (2)		
In Situ Pump	97		8.3	24.2	-26.7	±0.4 (6)		
In Situ Pump	120		4.9	25.2	-26.9	±0.4 (4)		
KOK-0303: *In situ* ^{13}C-Incubations								
Free-floating Array	40	40	9.0	25.2	-1.0	±0.1 (2)	1.05	0.12
Free-floating Array	80	80	8.8	24.6	-13.8	±0.2 (3)	0.50	0.06
Free-floating Array	100	100	4.0	24.6	-20.7	±0.3 (2)	0.11	0.03
Free-floating Array	120	120	2.7	25.2	-18.6	±0.4 (2)	0.10	0.04
KOK-0303: *In Situ* ^{13}C-Incubations (Depth Shift Experiments)								
Free-floating Array	120	40	10.3	24.3	87.1	±0.4 (3)	5.25	0.51
Free-floating Array	120	80	5.5	24.8	52.5	±0.4 (2)	1.94	0.35
Free-floating Array	120	100	1.9	23.2	7.0	±0.2 (2)	0.29	0.15
Free-floating Array	120	120	2.2	23.9	-12.9	(1)	0.14	0.06

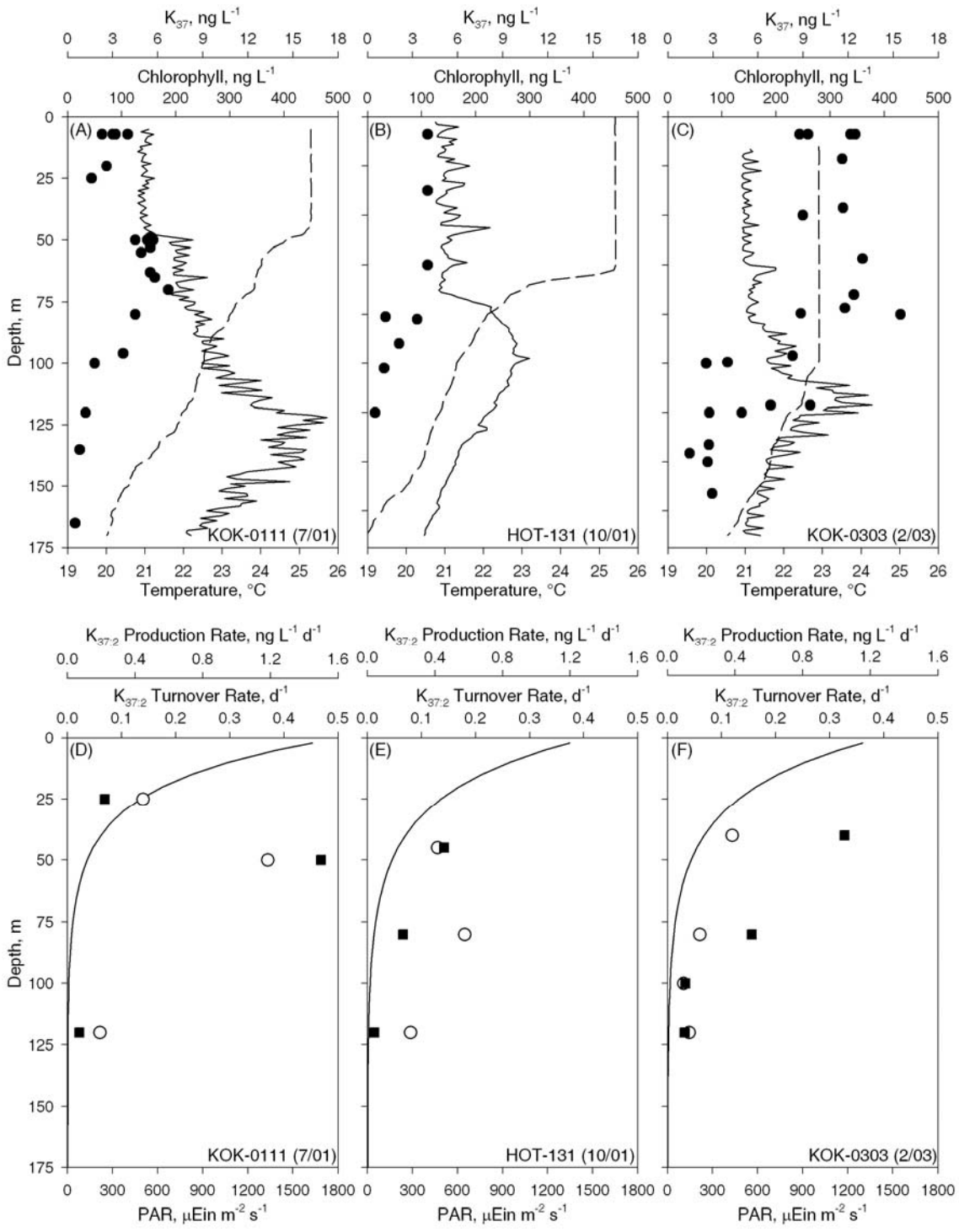
K37, ng L-1
Chlorophyll, ng L-1
(A)
(B)
(C)
KOK-0111 (7/01)
HOT-131 (10/01)
KOK-0303 (2/03)
Depth, m
Temperature, °C
K37:2 Production Rate, ng L-1 d-1
K37:2 Turnover Rate, d-1
(D)
(E)
(F)
PAR, µEin m-2 s-1

Figure 1

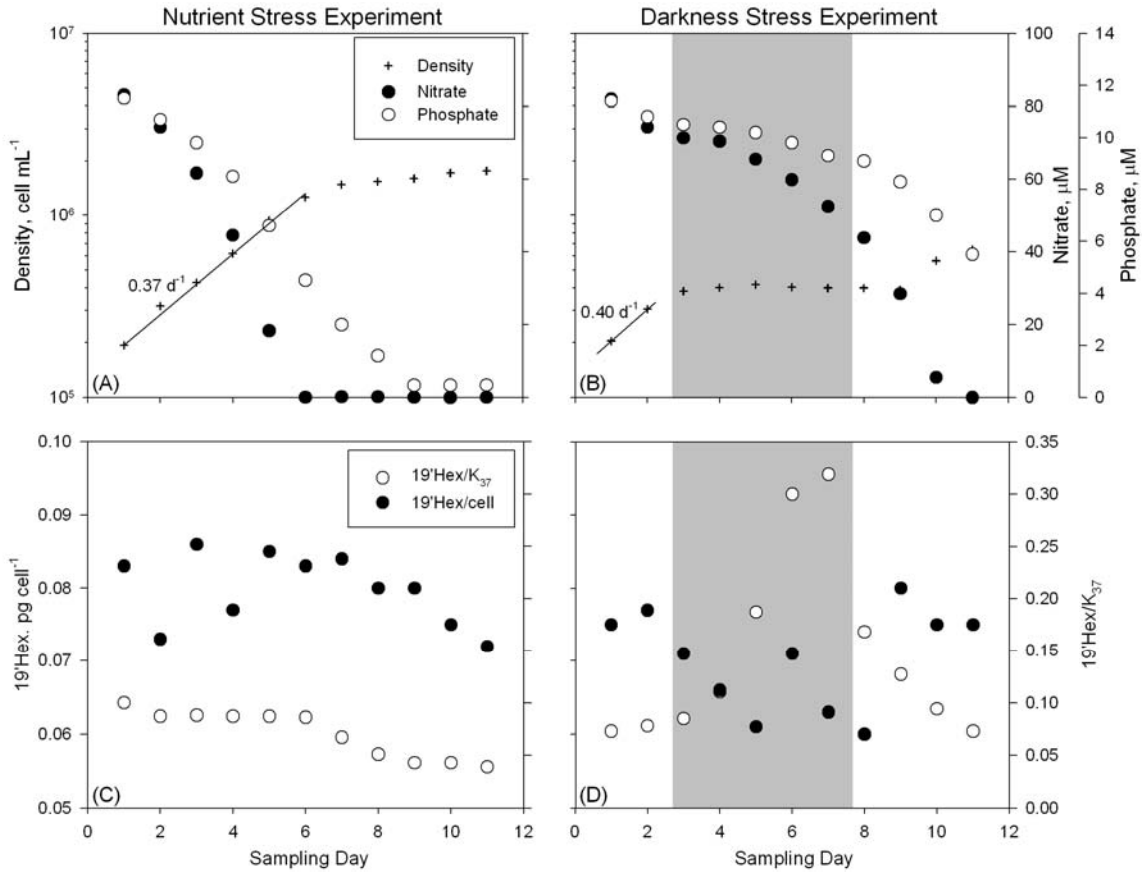
Nutrient Stress Experiment
Darkness Stress Experiment
Density
Nitrate
Phosphate
Density, cell mL-1
Nitrate, µM
Phosphate, µM
0.37 d-1
0.40 d-1
(A)
(B)
(C)
(D)
19'Hex/K37
19'Hex/cell
19'Hex. pg cell-1
19'Hex/K37
Sampling Day
Sampling Day

Figure 2

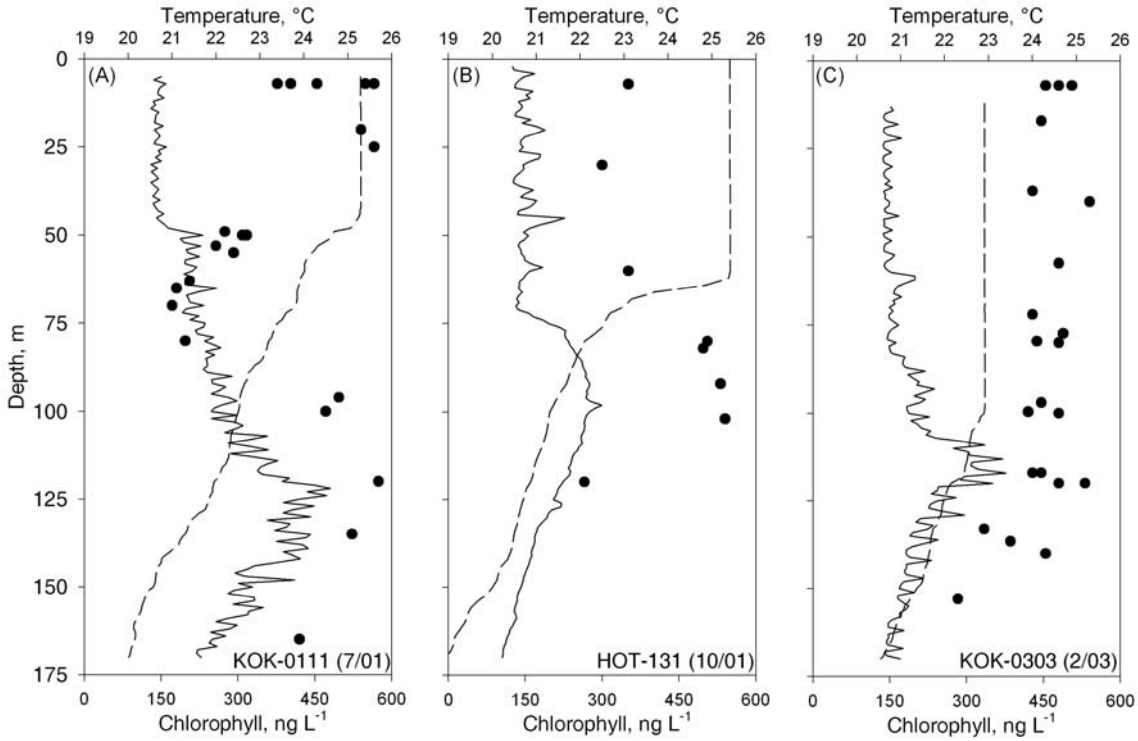
Temperature, °C
19 20 21 22 23 24 25 26
(A)
(B)
(C)
Depth, m
0 25 50 75 100 125 150 175
KOK-0111 (7/01)
HOT-131 (10/01)
KOK-0303 (2/03)
0 150 300 450 600
Chlorophyll, ng L-1

Figure 3

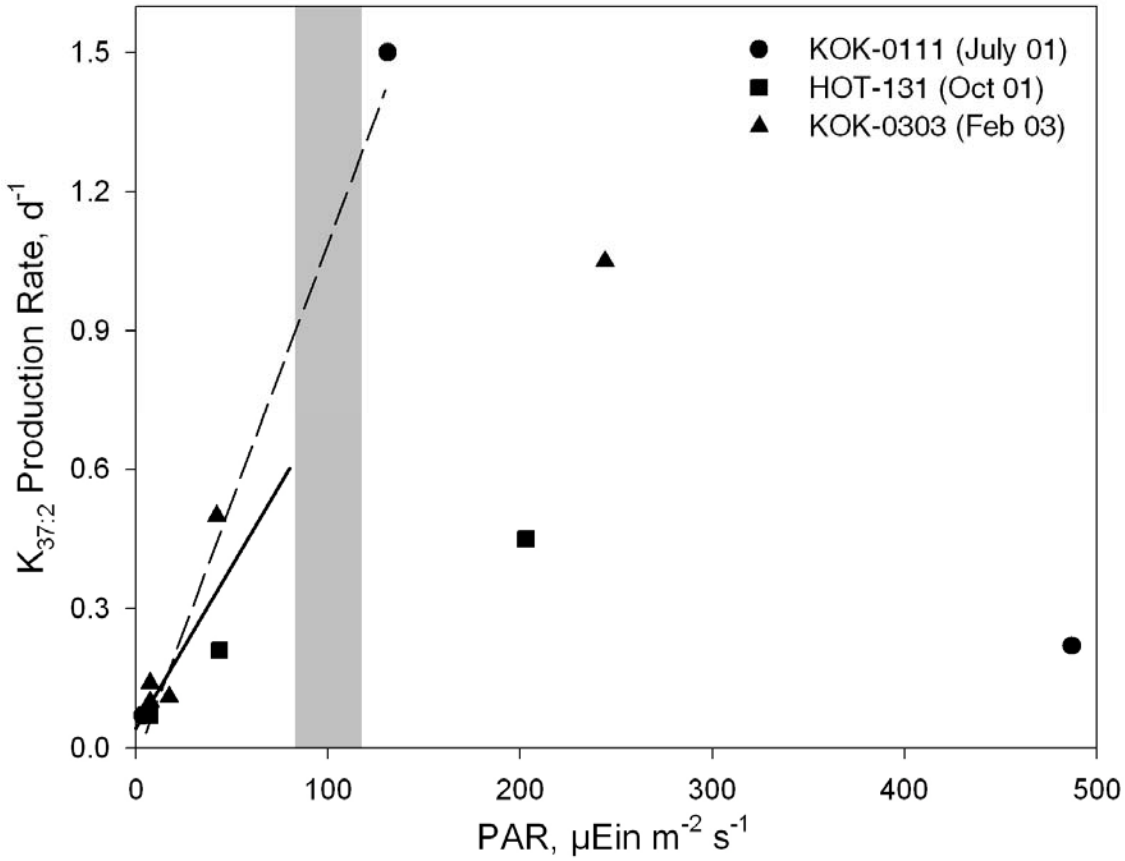
KOK-0111 (July 01)
HOT-131 (Oct 01)
KOK-0303 (Feb 03)
$K_{37:2}$ Production Rate, d^{-1}
PAR, µEin m^{-2} s^{-1}
0.0
0.3
0.6
0.9
1.2
1.5
0
100
200
300
400
500

Figure 4

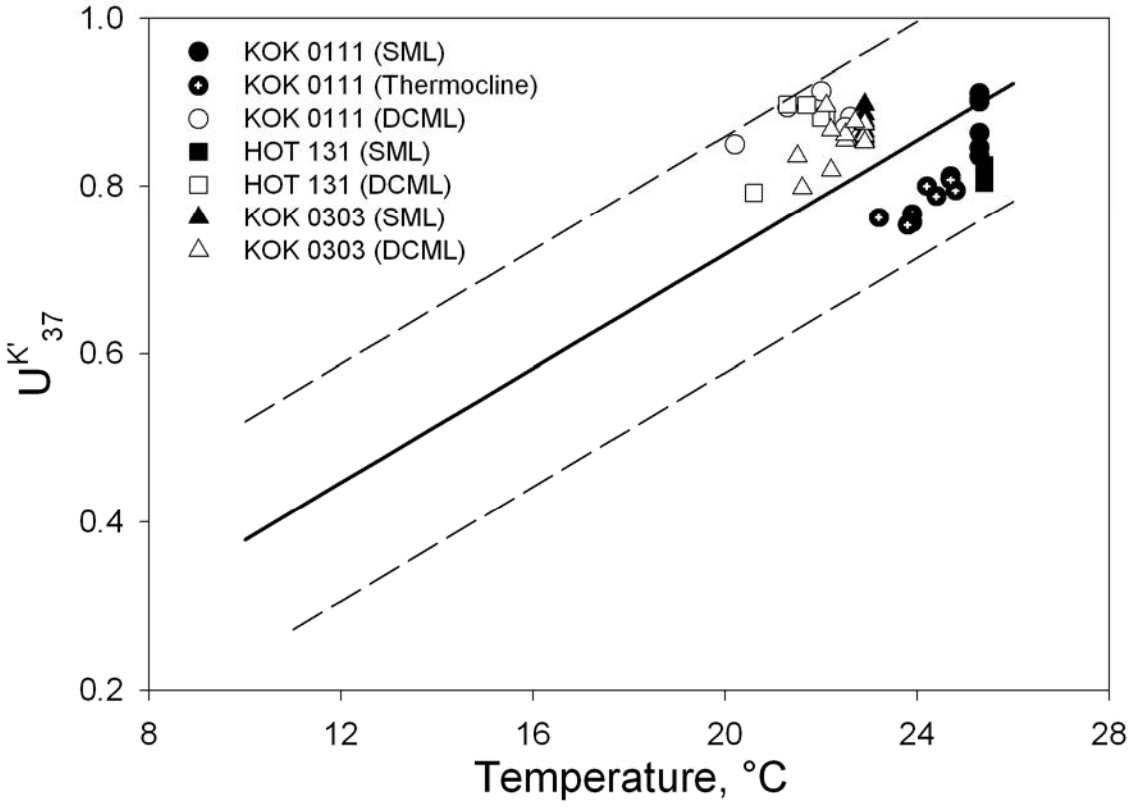
KOK 0111 (SML)
KOK 0111 (Thermocline)
KOK 0111 (DCML)
HOT 131 (SML)
HOT 131 (DCML)
KOK 0303 (SML)
KOK 0303 (DCML)
$U^{K'}_{37}$
1.0
0.8
0.6
0.4
0.2
8
12
16
20
24
28
Temperature, °C

Figure 5